

Comparison Between ^{18}F -FDG PET Image-Derived Indices for Early Prediction of Response to Neoadjuvant Chemotherapy in Breast Cancer

Mathieu Hatt¹, David Groheux^{2,3}, Antoine Martineau², Marc Espié⁴, Elif Hindié⁵, Sylvie Giacchetti⁴, Anne de Roquancourt⁶, Dimitris Visvikis¹, and Catherine Cheze-Le Rest^{1,7}

¹INSERM, UMR 1101 LaTIM, Brest, France; ²Department of Nuclear Medicine, Saint-Louis Hospital, Paris, France; ³B2T, Doctoral School, IUH, University of Paris VII, France; ⁴Breast Diseases Unit, Department of Medical Oncology, Saint-Louis Hospital, Paris, France; ⁵Department of Nuclear Medicine, Haut-Lévêque Hospital, University of Bordeaux, Bordeaux, France; ⁶Department of Pathology, Saint-Louis Hospital, Paris, France; and ⁷Department of Nuclear Medicine, CHU Milétrie, Poitiers, France

The goal of this study was to determine the best predictive factor among image-derived parameters extracted from sequential ^{18}F -FDG PET scans for early tumor response prediction after 2 cycles of neoadjuvant chemotherapy in breast cancer.

Methods: 51 breast cancer patients were included. Responder and nonresponder status was determined by histopathologic examination according to the tumor and node Sataloff scale. PET indices (maximum and mean standardized uptake value [SUV], metabolically active tumor volume, and total lesion glycolysis [TLG]), at baseline and their variation (Δ) after 2 cycles of neoadjuvant chemotherapy were extracted from the PET images. Their predictive value was investigated using Mann-Whitney *U* tests and receiver-operating-characteristic analysis. Subgroup analysis was also performed by considering estrogen receptor (ER)-positive/human epidermal growth factor receptor 2 (HER2)-negative, triple-negative, and HER2-positive tumors separately. The impact of partial-volume correction was also investigated using an iterative deconvolution algorithm.

Results: There were 24 pathologic nonresponders and 27 responders. None of the baseline PET parameters was correlated with response. After 2 neoadjuvant chemotherapy cycles, the reduction of each parameter was significantly associated with response, the best prediction of response being obtained with ΔTLG (96% sensitivity, 92% specificity, and 94% accuracy), which had a significantly higher area under the curve (0.91 vs. 0.82, $P = 0.01$) than did $\Delta\text{SUV}_{\text{max}}$ (63% sensitivity, 92% specificity, and 77% accuracy). Subgroup analysis confirmed a significantly higher accuracy for ΔTLG than ΔSUV for ER-positive/HER2-negative but not for triple-negative and HER2-positive tumors. Partial-volume correction had no impact on the predictive value of any of the PET image-derived parameters despite significant changes in their absolute values. **Conclusion:** Our results suggest that the reduction after 2 neoadjuvant chemotherapy cycles of the metabolically active volume of primary tumor measurements such as ΔTLG predicts histopathologic tumor response with higher accuracy than does ΔSUV measure-

ments, especially for ER-positive/HER2-negative breast cancer. These results should be confirmed in a larger group of patients as they may potentially increase the clinical value and efficiency of ^{18}F -FDG PET for early prediction of response to neoadjuvant chemotherapy.

Key Words: breast cancer; neoadjuvant chemotherapy; ^{18}F -FDG; tumor delineation; pathological response

J Nucl Med 2013; 54:341–349

DOI: 10.2967/jnumed.112.108837

Preoperative neoadjuvant chemotherapy has been used as standard treatment for inflammatory and nonoperable locally advanced breast carcinoma patients and is now increasingly being used for patients with operable but large breast tumors. This strategy allows patients to undergo breast-conserving surgery and provides information on the efficacy of chemotherapy (1). Early response prediction after 1 or 2 cycles of neoadjuvant chemotherapy might enable the selection of alternative treatment strategies (2). Breast carcinoma is a composite, and immunohistochemistry allows the definition of 3 main subgroups with different therapeutic responses and different outcomes (triple-negative, human epidermal growth factor receptor 2 (HER2)-positive, and luminal tumors). Pathologic complete response (pCR) is associated with a better outcome in the HER2-overexpressed and triple-negative breast cancer patients. On the other hand, recent studies showed that in luminal tumors, especially for luminal A, the impact of pCR on a patient's survival remains less established (3,4). Thus, an intermediate response with tumor shrinkage allowing breast-conserving surgery might be considered a reasonable clinical objective for this group.

Within this context, ^{18}F -FDG PET has been demonstrated to be a potent predictive tool (5–8). Indeed, correlations between the pathologic tumor response after completion of neoadjuvant chemotherapy and the decrease in tumor standardized uptake values (SUVs) after

Received Jun. 12, 2012; revision accepted Oct. 2, 2012.
For correspondence or reprints contact: Mathieu Hatt, INSERM, UMR 1101 LaTIM, CHRU Morvan, 5 Avenue Foch, 29609 Brest, France.
E-mail: hatt@univ-brest.fr
Published online Jan. 17, 2013.
COPYRIGHT © 2013 by the Society of Nuclear Medicine and Molecular Imaging, Inc.

1 or 2 courses of chemotherapy have been demonstrated in several studies. A recent metaanalysis (8) conducted on 19 studies including 920 patients for the early prediction of primary tumor response to neoadjuvant chemotherapy reported a pooled sensitivity of 84% and specificity of 66% in identifying responders. The authors emphasized that the low pooled specificity (66%) still calls for caution.

Most studies have considered SUV measurements only—mostly SUV_{max} , or SUV_{peak} averaging the SUV_{max} voxel with its neighboring voxels (9). On the other hand, it has been demonstrated in several recent studies and for various malignancies that other ^{18}F -FDG PET image-derived parameters can have a statistically significant higher predictive value than SUV in determining tumor response (10,11). These parameters, which allow for a more comprehensive tumor functional level evaluation, include metabolically active tumor volume (MATV) (11) and total lesion glycolysis (TLG), defined as the product of MATV and its associated SUV_{mean} (12). In a recent study that compared SUV_{max} and TLG derived using manual delineation and threshold, SUV_{max} had a better predictive value than TLG in identifying pCR (13).

To the best of our knowledge, no study has investigated the predictive value, regarding response to neoadjuvant chemotherapy for breast cancer, for all of the previously described ^{18}F -FDG PET image-derived parameters (SUV_{max} , SUV_{mean} , SUV_{peak} , TLG, MATV) within the same study, both at baseline and during treatment time points.

The current study was therefore conducted with the objective of determining the predictive value of several ^{18}F -FDG PET-derived parameters both at baseline and after 2 neoadjuvant chemotherapy cycles.

MATERIALS AND METHODS

Patient Population

The current study consisted of a retrospective analysis of a prospective cohort of 55 consecutive patients diagnosed with breast cancer and included in a previous clinical trial (14) performed after approval by the institutional ethical committee and with the patients' written informed consent. The PET/CT image datasets of 3 patients could not be retrieved from the database because of a corrupt archive file, and 1 was excluded from the analysis because of insufficient initial uptake (SUV_{max} , 1.5) in the primary tumor. Therefore, 51 patients were included in the retrospective analysis presented in this work (Table 1).

All patients underwent neoadjuvant chemotherapy with 4 cycles of epirubicin plus cyclophosphamide, followed by 4 cycles of docetaxel (plus trastuzumab in cases of HER2 overexpression [HER2-positive]). Patients underwent ^{18}F -FDG PET/CT scanning at baseline and after the second cycle of neoadjuvant chemotherapy (PET₁ and PET₂, respectively). At the completion of chemotherapy, all patients underwent surgery (mastectomy or lumpectomy).

^{18}F -FDG PET/CT Acquisitions

All ^{18}F -FDG PET/CT scans were obtained at Saint Louis Hospital in Paris between July 2007 and May 2009. A rigorous imaging protocol was designed to ensure robust SUV measurements

TABLE 1
Patient Characteristics

Characteristic	Number of patients
American Joint Committee on Cancer clinical stage*	
IIA	11 (21.5%)
IIB	13 (25.5%)
IIIA	12 (23.5%)
IIIB	14 (27.5%)
IIIC	1 (2%)
Tumor type	
Invasive ductal, no special type	45 (88%)
Metaplastic	3 (6%)
Lobular	3 (6%)
Grade	
1	4 (8%)
2	28 (55%)
3	17 (33%)
Unknown	2 (4%)
ER status[†]	
Positive	30 (59%)
Negative	21 (41%)
HER2 status[‡]	
Positive	12 (23.5%)
Negative	39 (76.5%)
Triple-negative status	
Triple-negative	13 (25.5%)
Not triple-negative	38 (74.5%)
Surgery	
Breast-conserving surgery	25 (49%)
Mastectomy	26 (51%)
Pathologic response	
Responders	27 (53%)
Nonresponders	24 (47%)

*Version 7 (16) according to clinical examination and conventional imaging findings.

[†]Tumors were considered positive for ER (estrogen receptor) if >10% of cells showed staining by immunohistochemistry.

[‡]Tumors were considered to be positive for HER2 if >30% of invasive tumor cells showed definite membrane staining resulting in so-called fishnet appearance.

across both time points. The blood glucose level had to be no more than 7 mmol/L. For both acquisitions, patients received an intravenous injection (in the arm opposite the breast tumor using a venous line) of ^{18}F -FDG (5 MBq/kg) after a fasting period of 6 h. After an uptake period of 60 min, all acquisitions were performed from mid-thigh level to the base of the skull with the arms raised, on a Gemini XL PET/CT system (Philips) that combines a germanium oxyorthosilicate-based PET scanner and a 16-slice Brilliance CT scanner. CT data were acquired first (120 kV, 100 mAs, no contrast enhancement). PET emission list-mode data were acquired in 3-dimensional (3D) mode, with 2 min per bed position, and reconstructed using a 3D row-action maximum-likelihood algorithm with a voxel size of 4 × 4 × 4 mm. The attenuation-corrected images were normalized for injected dose and body weight and converted into standardized uptake values (SUVs), defined as tracer concentration (kBq/mL)/(injected activity [kBq]/patient body weight [g]).

Tumor Histology and Immunohistochemistry Analysis

Tumor type was determined on the core-needle biopsy sample obtained before neoadjuvant chemotherapy. Immunohistochemical tests were performed on formalin-fixed, paraffin-embedded tissues, using specific antibodies and an automated immunostainer (XT Immunostainer; Ventana). Tumors were considered to be HER2-positive if more than 30% of invasive tumor cells showed definite membrane staining resulting in a so-called fishnet appearance; control by fluorescence in situ hybridization or silver-enhanced in situ hybridization was done for ambiguous cases. Tumors were considered estrogen receptor (ER)-negative or progesterone receptor-negative if there was less than 10% staining.

Three specific tumor subgroups as described previously were considered, namely triple-negative, ER-positive/HER2-negative (luminal), and HER2-positive.

Pathologic Tumor Response

Histopathologic response was assessed on surgical specimens at the completion of neoadjuvant chemotherapy. Response was graded in primary tumor (T) and nodes (N) according to the scale of Sataloff et al. (15), which was used in the frequently cited study by Rousseau et al. (6): TA = total or nearly total therapeutic effect, TB = greater than 50% therapeutic effect but less than total or nearly total effect, TC = less than 50% therapeutic effect but visible effect, TD = no therapeutic effect, NA = evidence of therapeutic effect and no residual disease, NB = no node metastases or therapeutic effect, NC = evidence of a therapeutic effect but metastasis still present, ND = metastasis still present and viable (no therapeutic effect). Complete and partial responders (T[A-B] with N[A-B-C]) were considered histopathologic responders, whereas patients with no response or progression (T[C-D], N[D]) were considered nonresponders.

The pCR rate, defined as absence of invasive cancer cells in the primary tumor and in lymph nodes (16), was also evaluated, and the predictive power of PET parameters to predict pCR was measured.

Investigated Parameters and Analysis

All PET image-derived parameters were extracted from the PET₁ and PET₂ images. For each patient, the primary tumor was identified on the PET image by a nuclear medicine physician with more than 10 y of experience and subsequently semiautomatically isolated in a 3D region of interest (ROI) containing the tumor and its surrounding background. Tumors were subsequently automatically delineated using the fuzzy locally adaptive bayesian (FLAB) algorithm (17) applied to the previously defined ROI. The FLAB approach allows automatic tumor delineation by computing a probability of belonging to a given class (e.g., tumor or background) for each voxel within the 3D ROI. This probability is calculated by taking into account the voxel's intensity with respect to the statistical distributions (characterized by their mean and variance) of the voxels in the various regions of the image, as well as its spatial correlation with neighboring voxels in 3 dimensions. This approach has been previously validated on simulated and clinical datasets for accuracy, robustness, and reproducibility, on both homogeneous and heterogeneous MATVs (17–19).

The potential impact of partial-volume effects was also investigated by correcting the image before analysis using a state-of-the-art iterative deconvolution previously validated for oncology PET applications (20). The analysis was subsequently performed on both the original and the partial-volume-effect-corrected images.

SUV_{max}, SUV_{peak}, and SUV_{mean}, as well as the MATV and the TLG, were then automatically calculated from the tumor delineations. SUV_{peak} was defined as the mean of voxel intensities in a 1.7-cm³ spheric ROI (27 voxels) centered on SUV_{max} (9). MATV was defined as the sum of all voxels contained in the FLAB-delineated volumes multiplied by the volume of a voxel (64 mm³). SUV_{mean} was defined as the mean of voxel intensities in the MATV delineated by FLAB. Subsequently, TLG was determined by multiplying the MATV and its associated SUV_{mean}. The percentage evolution of each parameter between baseline and after the second neoadjuvant chemotherapy cycle was calculated as (PET₂ parameter – PET₁ parameter)/PET₁ parameter × 100.

Statistical Analysis

Statistical analyses were performed using MedCalc (MedCalc Software). All parameters' distributions were expressed as median (or mean, depending on normality) ± SD and range. Normality was tested using the D'Agostino–Pearson test (21). For each parameter, its correlation with patient response was tested by determining the statistical difference between responders' and nonresponders' distributions using a Mann–Whitney *U* test. The absolute value of each parameter at PET₁ and PET₂ was investigated, as well as its evolution from PET₁ to PET₂. The predictive performance regarding the identification of responders was evaluated using receiver-operating-characteristic (ROC) analysis. Area under the curve (AUC), sensitivity, specificity, and accuracy were reported. Absolute and associated predictive parameter values extracted from the corrected PET images were compared with original ones. Subgroup analysis was also performed by considering triple-negative, HER2-positive, and ER-positive/HER2-negative tumors separately. All tests were 2-sided, and *P* values of 0.05 or less were considered statistically significant.

RESULTS

ER, progesterone receptor, and HER2 receptor status are provided in Table 1. Thirteen patients had triple-negative tumors, 12 had HER2-positive tumors, and 26 had ER-positive/HER2-negative tumors, which is representative (22). Considering the pathologic tumor response established at surgery (after completion of chemotherapy), there were 27 pathologic responders (53%) and 24 nonresponders (47%). pCR was found in 7 patients (13.7%), among which 3 had triple-negative and 4 had HER2-overexpressing tumors and 0 were ER-positive/HER2-negative. Figure 1 illustrates for a pathologic nonresponder and a responder the 2 scans, including delineation of the primary tumor.

Predictive Value of Parameters' Absolute Values

According to the D'Agostino–Pearson test, considering the entire patient cohort (*n* = 51), none of the parameters' absolute values at baseline and after the second cycle or associated variation (Δ) were normally distributed (Table 2). Similarly, the responder and nonresponder groups were not normally distributed (Fig. 2), except for the variation values (Fig. 3).

According to Mann–Whitney *U* tests, no significant correlation (*P* > 0.1) was observed between the baseline values and histopathologic response (Table 2), distributions of the parameters among responders and nonresponders being

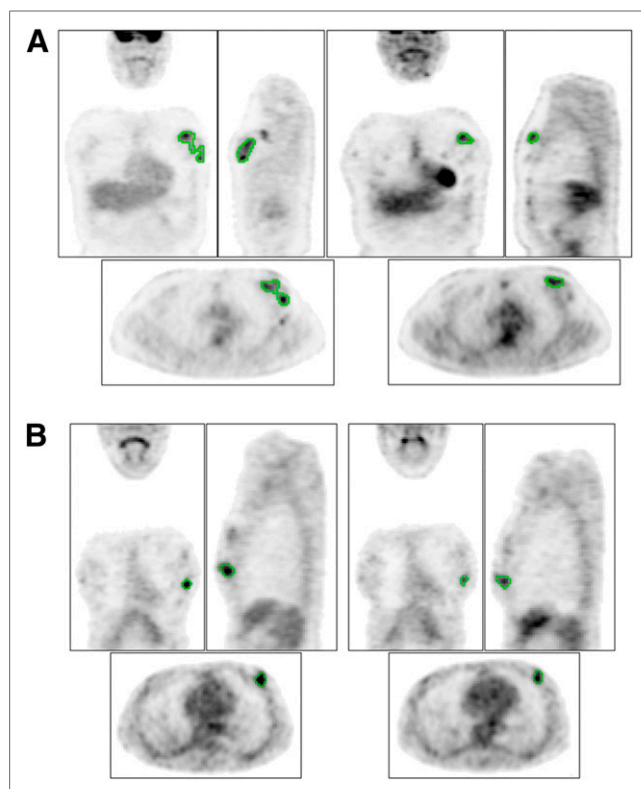


FIGURE 1. Illustration of PET₁ (left) and PET₂ (right) for pathologic responder (A) ($\Delta\text{SUV}_{\text{max}}$, -46% , ΔTLG , -89%) and nonresponder (B) (both $\Delta\text{SUV}_{\text{max}}$ and ΔTLG , -43%). Green contours represent FLAB delineation.

largely overlapped (Fig. 2A), leading to a low AUC of 0.52–0.63 (Table 3).

The primary tumors of nonresponders were characterized by a higher PET₂ SUV_{max} (5.3 ± 6.2 vs. 2.8 ± 2.9 , $P = 0.04$) and TLG (30 ± 160 vs. 14 ± 13 , $P = 0.05$). However, no correlation ($P \geq 0.07$) was found for any of the other parameters considered (Table 2).

For all parameters, the distributions were largely overlapped (Figs. 2A–2C), as the results of ROC analysis demonstrate, with a low AUC of 0.62–0.67 (Table 3). For SUV, sensitivity (57%–69%) and specificity (71%–75%) were limited. On the other hand, for volume-based measure-

ments, sensitivity was higher (89% and 78% for MATV and TLG, respectively) but specificity was lower (42% and 63% for MATV and TLG, respectively).

Evolution of Parameters and Associated Predictive Value

There was a global trend of decreasing MATV and associated tumors' uptake after the first 2 neoadjuvant chemotherapy cycles, although for some patients PET image-derived parameters were also found to be increasing (Table 2). The lowest and largest decreases were observed for $\Delta\text{SUV}_{\text{max}}$ ($-34\% \pm 32\%$) and ΔTLG ($-59\% \pm 34\%$), respectively.

According to Mann–Whitney U tests, the variation of all parameters was statistically different between responders and nonresponders, especially for ΔMATV and ΔTLG ($P < 0.0001$), as well as $\Delta\text{SUV}_{\text{max}}$ ($P = 0.0001$) (Table 2).

According to ROC analysis, the best prediction was achieved using the ΔTLG , with a sensitivity of 96% and specificity of 92%, resulting in an accuracy of 94% (Table 3). The ΔMATV was also an accurate predictive factor (sensitivity, 93%; specificity, 88%; accuracy, 91%). On the other hand, ΔSUV measurements led to significantly lower AUCs (0.68 for $\Delta\text{SUV}_{\text{mean}}$ to 0.82 for $\Delta\text{SUV}_{\text{max}}$ vs. 0.92 for ΔMATV and 0.91 for ΔTLG , $P \leq 0.01$) (Fig. 4A), with significantly lower sensitivity (63%–74%), specificity (67%–92%), and resulting accuracy (71%–77%) (Table 3). The least overlapped distributions were those associated with ΔMATV and ΔTLG (Fig. 3). The optimal cutoff values maximizing sensitivity and specificity were -48% , -42% , -30% , -42% , and -56% for $\Delta\text{SUV}_{\text{max}}$, $\Delta\text{SUV}_{\text{peak}}$, $\Delta\text{SUV}_{\text{mean}}$, ΔMATV , and ΔTLG , respectively (Table 3, Fig. 3).

Tumor Subgroup Analysis

When considering ER-positive/HER2-negative patients ($n = 26$), all AUCs were slightly higher but with the same hierarchy as for the entire cohort: ΔTLG and ΔMATV resulted in AUCs of 0.96 and 0.98, respectively, whereas ΔSUV measurements led to AUCs of 0.69, 0.84, and 0.88 for $\Delta\text{SUV}_{\text{mean}}$, $\Delta\text{SUV}_{\text{peak}}$, and $\Delta\text{SUV}_{\text{max}}$, respectively.

The ROC analysis performed on the 12 HER2-positive and 13 triple-negative breast cancer patients resulted in

TABLE 2
PET Parameter Values and Correlation with Response

Parameter	PET ₁	<i>P</i>	PET ₂	<i>P</i>	$\Delta(\text{PET}_1, \text{PET}_2)$ (%)	<i>P</i>
SUV_{max}	6.8 (2.3, 27.5)	0.8	3.9 (1.4, 30.7)	0.04*	-34 ($-90, +104$)	0.0001*
SUV_{peak}	4.8 (1.9, 22.0)	0.8	2.9 (1.0, 24.5)	0.07	-39 ($-90, +73$)	0.0004*
SUV_{mean}	3.7 (1.3, 18.7)	0.7	2.5 (1.0, 17.9)	0.2	-36 ($-87, +69$)	0.026*
MATV (cm ³)	14 (2, 227)	0.1	7 (1, 154)	0.09	-45 ($-89, +74$)	<0.0001*
TLG	51 (9, 668)	0.4	16 (1, 758)	0.05*	-59 ($-98, +51$)	<0.0001*

*Statistically significant.

Data are median, with minimum and maximum in parentheses.

P values are for responders vs. nonresponders, as determined using Mann–Whitney U test.

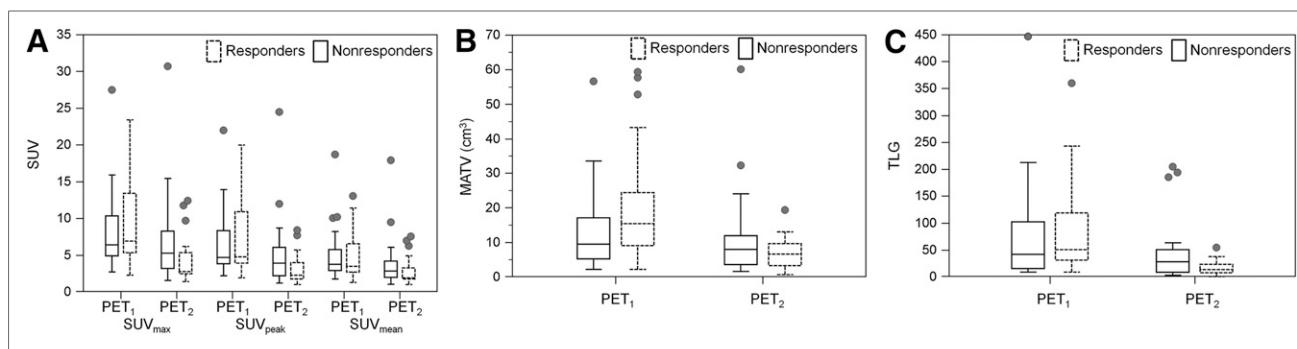


FIGURE 2. Box-and-whisker distribution plots of SUV_{max}, SUV_{peak}, and SUV_{mean} (A); MATV (B); and TLG (C) absolute values at PET₁ and PET₂. One patient with extremely high MATV and TLG values does not appear for readability purposes. Central box represents values from 25th to 75th percentiles. Middle line represents median. A line extends from minimum to maximum, excluding outliers, which are displayed as separate points.

nonstatistically significant different AUCs for volume-based measurements and SUVs ($P > 0.05$) in both cases.

Prediction of pCR

The pCR predictive value of all parameters was reduced with respect to the prediction of partial response. The hierarchy was, however, similar, with AUCs of 0.76, 0.79, 0.67, 0.63, and 0.59 for Δ TLG, Δ MATV, Δ SUV_{max}, Δ SUV_{peak}, and Δ SUV_{mean}, respectively (Fig. 5A).

Impact of Partial-Volume-Effect Correction

The correction of partial-volume effects had no significant impact on the resulting variation of either SUV or volume-based parameters, despite the significant impact on their PET₁ and PET₂ absolute values. There were therefore no statistically significant differences between the AUCs of ROC curves generated using $\Delta(\%)$ calculated using the original and corrected PET image-derived parameters (Figs. 4B and 5B).

DISCUSSION

The current study was the first, to our knowledge, investigation into the predictive value of ¹⁸F-FDG PET-derived parameters on a breast cancer cohort, including MATV, TLG, and 3 different SUV measurements at baseline and their evolution. Our results contradict those of the only other study to date comparing the performance of Δ SUV_{max} and Δ TLG—a study that reported a higher predictive value for Δ SUV_{max} (13). In that previous study, Δ SUV_{mean}, Δ SUV_{peak}, and Δ MATV predictive values were not considered. In addition, Δ TLG values were derived from tumor volumes delineated through manual contouring using a fixed threshold. Such a delineation approach has been previously shown to be inaccurate for PET (23,24). In our study, a previously validated robust and reproducible MATV segmentation algorithm was used. Another difference is that results in the previously reported study were reported for the prediction of pCR only, corresponding to 17% of the 142 patients, with a resulting cutoff Δ SUV_{max} of 83%–88%, which led to high specificity (96%) but low sensitivity (67%). In our study, we considered as pathologic responders patients with complete or partial

response in the primary breast cancer and lymph nodes. According to this criterion we found that MATV and TLG were more predictive than SUV. We refined a subsequent analysis considering pCR only for responders, and we observed also that volume parameters were superior (AUC, 0.76–0.79) to SUV (0.59–0.67).

In contrast to results for several malignancies such as locally advanced esophageal cancer (11) or non-Hodgkin lymphoma (10), none of the absolute baseline values (with or without correction) was significantly associated with response. The absolute values of some parameters (SUV_{max} and TLG) after the second cycle (PET₂) were significantly correlated with response but had limited predictive value. The most powerful predictive factors were the evolution between the baseline and the second scan.

Pathologic responders were associated with a significantly higher decrease in the ¹⁸F-FDG PET-derived indices considered. Among these, Δ TLG and Δ MATV were the best predictive factors compared with Δ SUV measurements, with significantly higher accuracy (91% and 94% for MATV and TLG vs. 71%, 76%, and 77% for Δ SUV_{mean}, Δ SUV_{peak} and Δ SUV_{max}, respectively). With respect to the recent metaanalysis that reported an overall 84% sensitivity and 66% specificity based on Δ SUV_{max} (8), our Δ SUV_{max} results demonstrated lower sensitivity (63%) but higher specificity (92%), whereas Δ TLG resulted in both higher sensitivity (96%) and higher specificity (92%). The metaanalysis also demonstrated large differences in sensitivities and specificities among the various considered studies due to combinations of different patient populations, response criteria (pCR or partial response), and cutoff values. Our study is in line with previous findings that the reduction of PET indices after 2 cycles is a good predictor of response to neoadjuvant chemotherapy in breast cancer (8). We further demonstrated the added value of considering more complete tumor characterization in ¹⁸F-FDG PET images through the delineation of the MATV over SUV measurements only. On the one hand, these results were mostly unchanged when the analysis was performed on the subgroup

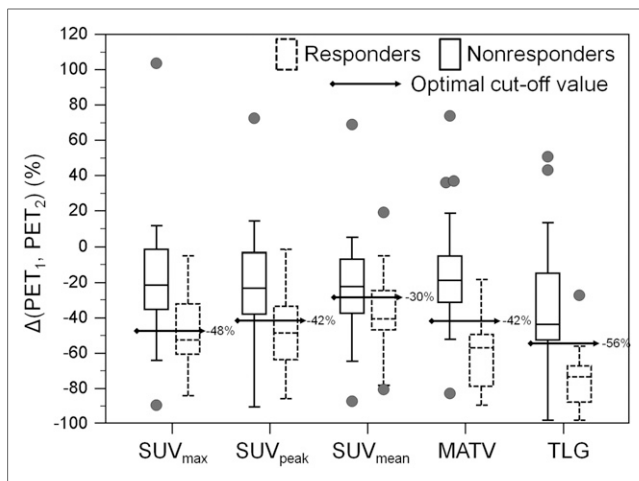


FIGURE 3. Box-and-whisker distribution plots of $\Delta\text{SUV}_{\text{max}}$, $\Delta\text{SUV}_{\text{peak}}$, $\Delta\text{SUV}_{\text{mean}}$, ΔMATV , and ΔTLG . Optimal cutoffs providing best accuracy in predicting response are displayed. Central box represents values from 25th to 75th percentiles. Middle line represents median. A line extends from minimum to maximum, excluding outliers, which are displayed as separate points.

of ER-positive/HER2-negative patients. On the other hand, the respective predictive values of ΔSUV , ΔMATV , and ΔTLG were similar for the triple-negative and HER2-positive breast cancer patients. However, since this subgroup analysis included a small number of patients (13 triple-negative and 12 HER2-positive), it needs to be further validated in a larger patient population. Future validation studies on larger groups of patients will be focused on ER-positive/HER2-negative patients since it is for this subgroup that the added value of ΔMATV and ΔTLG over ΔSUV seems to be the most significant. This observation can be explained by the fact that ER-positive/HER2-negative tumors are known to exhibit lower initial ^{18}F -FDG uptake

and therefore have lower decrease margins (7,25,26). These tumors are also known to only partially respond to neoadjuvant chemotherapy, requiring finer characterization of their response (27,28). Therefore, the addition of functional tumor volume-based metrics logically improves predictive accuracy for these tumors. For triple-negative and HER2-positive tumors that exhibit higher ^{18}F -FDG uptake and associated decrease margins, as well as better pCR rates, the addition of volume-based metrics might not translate into a significantly improved predictive value over ΔSUV measurements.

Another interesting result of our study was that $\Delta\text{SUV}_{\text{mean}}$ had significantly lower predictive value than $\Delta\text{SUV}_{\text{peak}}$ and $\Delta\text{SUV}_{\text{max}}$ (AUC of 0.68 vs. 0.79 and 0.82, respectively, $P < 0.02$). Considering the use of $\Delta\text{SUV}_{\text{peak}}$ relative to $\Delta\text{SUV}_{\text{max}}$, as proposed by the PERCIST recommendations (9), in this study there were no statistically significant differences between the two (AUC, 0.79 vs. 0.82, $P = 0.2$), despite $\Delta\text{SUV}_{\text{max}}$ leading to slightly better results than $\Delta\text{SUV}_{\text{peak}}$. Both these parameters describe the highest-activity region of the tumor, whereas the mean value is a better representative measurement of the entire tumor. A potential explanation for the lower predictive value of $\Delta\text{SUV}_{\text{mean}}$ is its higher dependency on partial-volume effects compared with SUV_{max} and SUV_{peak} . It has, however, recently been shown in a group of 15 breast cancer patients that correction of partial-volume effect had limited impact on SUV reduction (29), without reporting, however, on the actual impact of this reduction on the overall response predictive value. Another study investigated the impact of correction on the prediction of response to neoadjuvant chemotherapy for breast cancer using dynamic ^{18}F -FDG PET. The investigators found that correction eliminated significant differences in percentage ^{18}F -FDG uptake measurement changes for nonresponders (NR) versus partial responders but not for pCR versus other response categories (30). In the aforementioned work, partial-volume

TABLE 3
Predictive Value According to ROC Analysis

Parameter	Timing	AUC	Cutoff value	Sensitivity (%)	Specificity (%)	Accuracy (%)
SUV_{max}	PET ₁	0.52 [0.37–0.66]	>11.6	30 [14–50]	83 [63–95]	55 [38–68]
	PET ₂	0.67 [0.52–0.79]	≤3.7	67 [46–84]	75 [53–90]	71 [49–87]
	Δ (%)	0.82 [0.68–0.91]	≤−48	63 [42–81]	92 [73–99]	77 [57–90]
SUV_{peak}	PET ₁	0.52 [0.37–0.66]	>11.7	22 [9–42]	88 [68–97]	53 [34–69]
	PET ₂	0.65 [0.50–0.78]	≤2.8	63 [42–81]	71 [49–87]	67 [46–85]
	Δ (%)	0.79 [0.65–0.89]	≤−42	70 [50–86]	83 [63–95]	76 [54–91]
SUV_{mean}	PET ₁	0.53 [0.38–0.67]	≤2.2	19 [6–38]	92 [73–99]	53 [34–69]
	PET ₂	0.62 [0.47–0.75]	≤2	59 [39–78]	75 [53–90]	67 [46–85]
	Δ (%)	0.68 [0.54–0.81]	≤−30	74 [54–89]	67 [45–84]	71 [49–88]
MATV (cm ³)	PET ₁	0.63 [0.48–0.76]	>7	85 [66–96]	42 [22–63]	65 [48–79]
	PET ₂	0.64 [0.49–0.77]	≤11.3	89 [71–98]	42 [22–63]	67 [45–84]
	Δ (%)	0.92 [0.82–0.98]	≤−42	93 [76–99]	88 [68–97]	91 [72–98]
TLG	PET ₁	0.57 [0.43–0.71]	>16	93 [76–99]	29 [13–51]	63 [42–81]
	PET ₂	0.66 [0.51–0.79]	≤23.3	78 [58–91]	63 [41–82]	71 [49–88]
	Δ (%)	0.91 [0.79–0.97]	≤−56	96 [81–100]	92 [73–99]	94 [79–99]

Data in brackets are 95% confidence intervals.

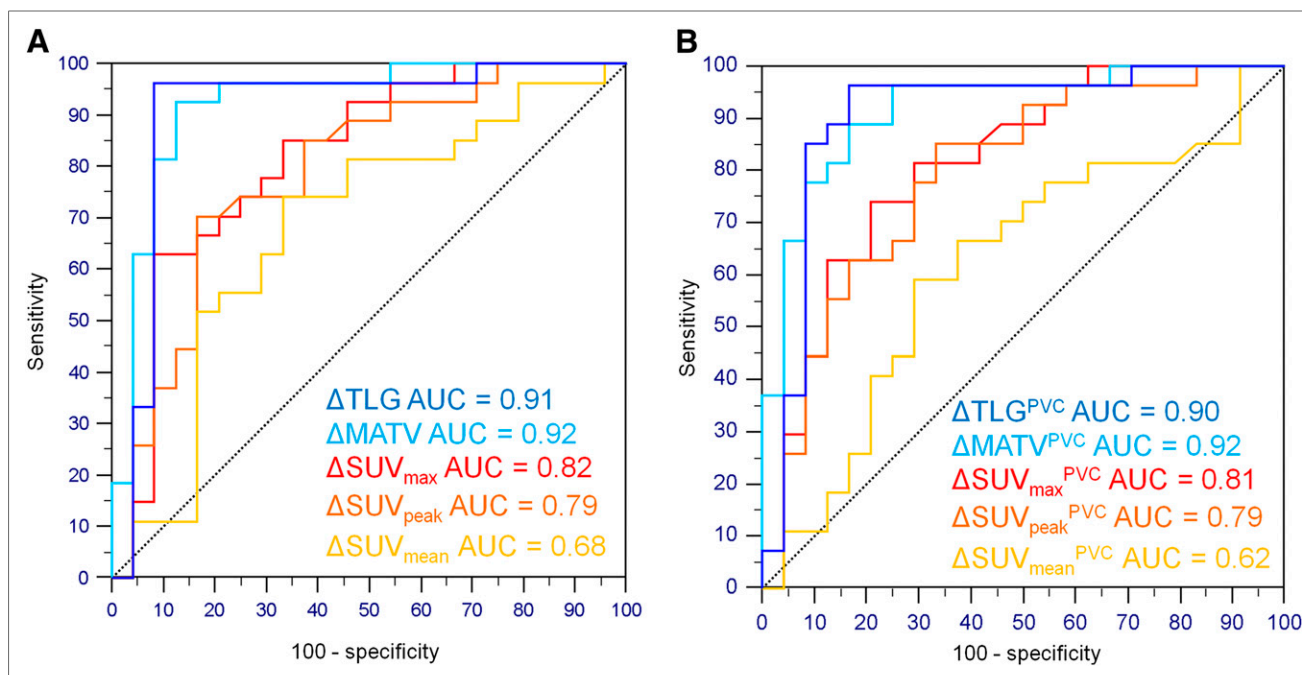


FIGURE 4. ROC curves related to prediction of responders for $\Delta\text{SUV}_{\text{max}}$, $\Delta\text{SUV}_{\text{peak}}$, $\Delta\text{SUV}_{\text{mean}}$, ΔMATV , and ΔTLG without (A) or with (B) partial-volume effect correction.

effect was corrected using simplistic recovery coefficients, applied only to tumors smaller than 3 cm based on MR imaging. In our study, correction was systematically applied to all images using a voxelwise iterative image deconvolution algorithm previously validated for PET images (20). In this work, the use of correction did not change either the

predictive value of the parameters or their evolution or the statistical differences between groups of response, despite a significant change in their absolute values. Finally, correction did not improve the predictive value of SUV_{mean} or the hierarchy of performance between the 3 different SUV measurements, for either the partial or the pCR response criteria.

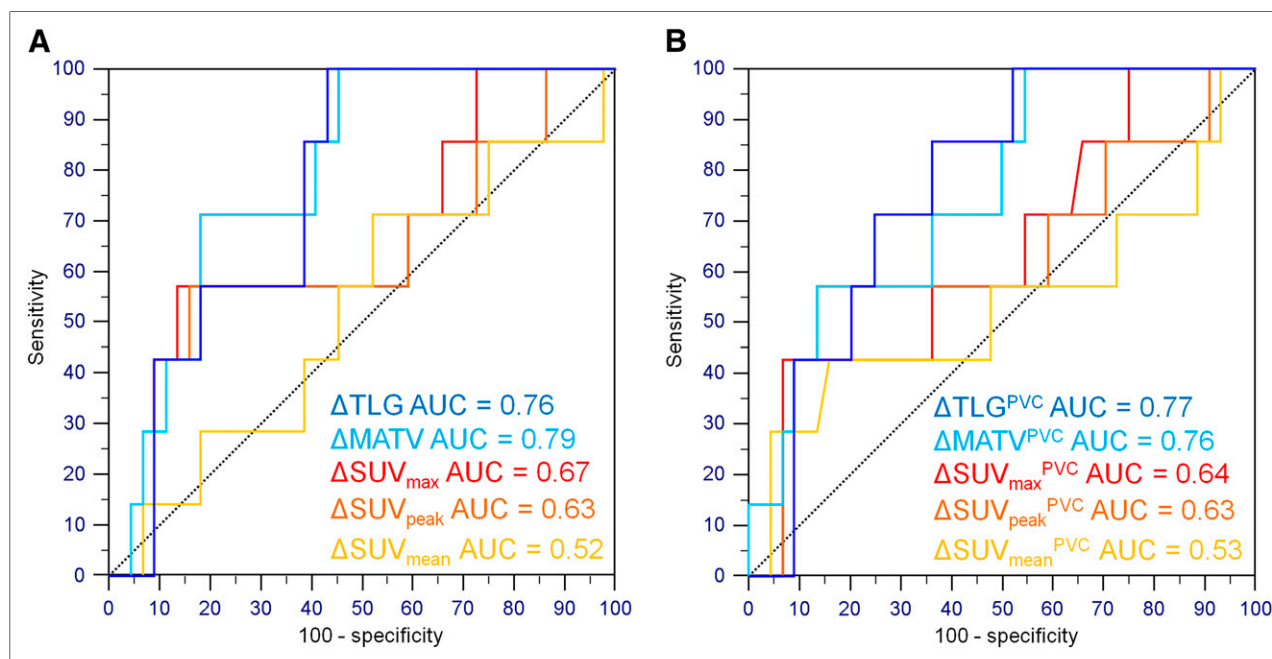


FIGURE 5. ROC curves related to prediction of pCR for $\Delta\text{SUV}_{\text{max}}$, $\Delta\text{SUV}_{\text{peak}}$, $\Delta\text{SUV}_{\text{mean}}$, ΔMATV , and ΔTLG without (A) or with (B) partial-volume effect correction.

This lack of correction impact is consistent with our previous findings (31,32).

The delineation of breast cancer MATVs is challenging because they often exhibit heterogeneous uptake distributions and complex shapes or low tumor-to-background ratios, particularly in the midtreatment scan. Therefore, the use of a robust algorithm is recommended. Within this context, the results presented here using FLAB may be replicated using alternative approaches, such as gradient-based (33) or improved fuzzy C-means (34) methods. Using less robust approaches might lead to significant differences in the results concerning the value of volume-derived parameters (11,13). In addition, this effect may be more important when the temporal evolution of such parameters is considered, as measurements have to be considered with respect to the known physiologic reproducibility ranges. Differences have to be larger than $\pm 30\%$ to characterize response, because of the upper and lower physiologic reproducibility limits associated with PET-derived measurements (19). Considering MATV and TLG values, these reproducibility limits were obtained using the FLAB method, whereas less robust approaches (fixed and adaptive threshold) lead to larger values ($\pm 50\%$ – 90%) (19). The FLAB method also allows for measurements that are more repeatable, with low inter- and intraobserver variability (18,19). Finally, the imaging protocol in this study was specifically designed to ensure robust and reproducible tumor characterization between both time points. For most patients, measured evolutions were outside the reproducibility limits. Optimal cutoffs were also larger: -48% for SUV_{max} , which is in accordance with previous findings (8), and -42% and -56% for MATV and TLG, respectively.

One potential limitation of this study was its retrospective nature and the resulting potential bias, and the lack of reliable outcome information due to the short delay between surgery and last follow-up. Another limitation was the relatively small number of patients due to the fact that the previous prospective study was limited to 55 patients (14), 4 of whom could not be included in the present study. This small sample is especially restrictive regarding the subgroup analyses of triple-negative and HER2-positive patients. The findings of this study therefore need to be validated in larger patient cohorts. Another limitation was that although nodal status was considered to define pathologic response, only primary tumors were characterized in the images to simplify the analysis. Finally, some of the patients were characterized by ΔTLG and $\Delta MATV$ decreases that were close to the optimal cutoffs but sufficient to avoid misclassification, whereas the opposite was true for SUV_{max} (Figs. 3). The statistical difference between AUCs of ΔSUV_{max} and ΔTLG might therefore be lower in larger prospective studies. However, values of $\Delta MATV$ and ΔTLG present a higher spread than ΔSUV measurements as demonstrated in Figure 3, showing their higher discriminative power as demonstrated by Mann–Whitney U tests (Table 2).

CONCLUSION

The reduction of metabolically active primary tumor volumes and associated activity measurements such as TLG after 2 neoadjuvant chemotherapy cycles predicts histopathologic tumor response with statistically significant higher accuracy (94%) than SUV_{max} (77%). The advantage of TLG over SUV_{max} was particularly evident for the 26 patients in the ER-positive/HER2-negative subgroup, and therefore we will focus on confirming these results in a larger group of ER-positive/HER2-negative patients. Such confirmation may potentially increase the clinical value and efficiency of ^{18}F -FDG PET for early prediction of response to neoadjuvant chemotherapy.

DISCLOSURE

The costs of publication of this article were defrayed in part by the payment of page charges. Therefore, and solely to indicate this fact, this article is hereby marked “advertisement” in accordance with 18 USC section 1734. No potential conflict of interest relevant to this article was reported.

REFERENCES

1. Fisher B, Bryant J, Wolmark N, et al. Effect of preoperative chemotherapy on the outcome of women with operable breast cancer. *J Clin Oncol*. 1998;16:2672–2685.
2. Groheux D, Giacchetti S, Espie M, Rubello D, Moretti JL, Hindie E. Early monitoring of response to neoadjuvant chemotherapy in breast cancer with ^{18}F -FDG PET/CT: defining a clinical aim. *Eur J Nucl Med Mol Imaging*. 2011;38:419–425.
3. Bhargava R, Beriwal S, Dabbs DJ, et al. Immunohistochemical surrogate markers of breast cancer molecular classes predicts response to neoadjuvant chemotherapy: a single institutional experience with 359 cases. *Cancer*. 2010;116:1431–1439.
4. von Minckwitz G, Untch M, Blohmer JU, et al. Definition and impact of pathologic complete response on prognosis after neoadjuvant chemotherapy in various intrinsic breast cancer subtypes. *J Clin Oncol*. 2012;30:1796–1804.
5. Groheux D, Hindie E, Giacchetti S, et al. Triple-negative breast cancer: early assessment with ^{18}F -FDG PET/CT during neoadjuvant chemotherapy identifies patients who are unlikely to achieve a pathologic complete response and are at a high risk of early relapse. *J Nucl Med*. 2012;53:249–254.
6. Rousseau C, Devillers A, Sagan C, et al. Monitoring of early response to neoadjuvant chemotherapy in stage II and III breast cancer by [^{18}F]fluorodeoxyglucose positron emission tomography. *J Clin Oncol*. 2006;24:5366–5372.
7. Schwarz-Dose J, Untch M, Tiling R, et al. Monitoring primary systemic therapy of large and locally advanced breast cancer by using sequential positron emission tomography imaging with [^{18}F]fluorodeoxyglucose. *J Clin Oncol*. 2009;27:535–541.
8. Wang Y, Zhang C, Liu J, Huang G. Is ^{18}F -FDG PET accurate to predict neoadjuvant therapy response in breast cancer? A meta-analysis. *Breast Cancer Res Treat*. 2012;131:357–369.
9. Wahl RL, Jacene H, Kasamon Y, Lodge MA. From RECIST to PERCIST: evolving considerations for PET response criteria in solid tumors. *J Nucl Med*. 2009;50(suppl 1):122S–150S.
10. Cazaentre T, Morschhauser F, Vermandel M, et al. Pre-therapy ^{18}F -FDG PET quantitative parameters help in predicting the response to radioimmunotherapy in non-Hodgkin lymphoma. *Eur J Nucl Med Mol Imaging*. 2010;37:494–504.
11. Hatt M, Visvikis D, Pradier O, Cheze-le Rest C. Baseline ^{18}F -FDG PET image-derived parameters for therapy response prediction in oesophageal cancer. *Eur J Nucl Med Mol Imaging*. 2011;38:1595–1606.
12. Larson SM, Erdi Y, Akhurst T, et al. Tumor treatment response based on visual and quantitative changes in global tumor glycolysis using PET-FDG imaging: the visual response score and the change in total lesion glycolysis. *Clin Positron Imaging*. 1999;2:159–171.
13. Tateishi U, Miyake M, Nagaoka T, et al. Neoadjuvant chemotherapy in breast cancer: prediction of pathologic response with PET/CT and dynamic contrast-enhanced MR imaging—prospective assessment. *Radiology*. 2012;263:53–63.

14. Groheux D, Moretti J, Espié M, et al. FDG PET/CT for early prediction of the response of neoadjuvant chemotherapy for breast cancer after two courses of EC (epirubicin + cyclophosphamide) [abstract]. *J Nucl Med*. 2010;51(suppl 2):51P.
15. Sataloff DM, Mason BA, Prestipino AJ, Seinige UL, Lieber CP, Baloch Z. Pathologic response to induction chemotherapy in locally advanced carcinoma of the breast: a determinant of outcome. *J Am Coll Surg*. 1995;180:297–306.
16. Edge SB, Compton CC. The American Joint Committee on Cancer: the 7th ed. of the AJCC cancer staging manual and the future of TNM. *Ann Surg Oncol*. 2010;17:1471–1474.
17. Hatt M, Cheze le Rest C, Descourt P, et al. Accurate automatic delineation of heterogeneous functional volumes in positron emission tomography for oncology applications. *Int J Radiat Oncol Biol Phys*. 2010;77:301–308.
18. Hatt M, Cheze Le Rest C, Albarghach N, Pradier O, Visvikis D. PET functional volume delineation: a robustness and repeatability study. *Eur J Nucl Med Mol Imaging*. 2011;38:663–672.
19. Hatt M, Cheze-Le Rest C, Aboagy EO, et al. Reproducibility of ^{18}F -FDG and 3'-deoxy-3'- ^{18}F -fluorothymidine PET tumor volume measurements. *J Nucl Med*. 2010;51:1368–1376.
20. Boussion N, Cheze Le Rest C, Hatt M, Visvikis D. Incorporation of wavelet-based denoising in iterative deconvolution for partial volume correction in whole-body PET imaging. *Eur J Nucl Med Mol Imaging*. 2009;36:1064–1075.
21. Sheskin D. *Handbook of Parametric and Nonparametric Statistical Procedures*. 5th ed. Boca Raton, FL: Chapman & Hall/CRC; 2011.
22. Straver ME, Rutgers EJ, Rodenhuis S, et al. The relevance of breast cancer subtypes in the outcome of neoadjuvant chemotherapy. *Ann Surg Oncol*. 2010;17:2411–2418.
23. Hatt M, Cheze-le Rest C, van Baardwijk A, Lambin P, Pradier O, Visvikis D. Impact of tumor size and tracer uptake heterogeneity in ^{18}F -FDG PET and CT non-small cell lung cancer tumor delineation. *J Nucl Med*. 2011;52:1690–1697.
24. Hatt M, Visvikis D, Le Rest CC. Autocontouring versus manual contouring [letter]. *J Nucl Med*. 2011;52:658.
25. McDermott GM, Welch A, Staff RT, et al. Monitoring primary breast cancer throughout chemotherapy using FDG-PET. *Breast Cancer Res Treat*. 2007;102:75–84.
26. Groheux D, Giacchetti S, Moretti JL, et al. Correlation of high ^{18}F -FDG uptake to clinical, pathological and biological prognostic factors in breast cancer. *Eur J Nucl Med Mol Imaging*. 2011;38:426–435.
27. Lips EH, Mulder L, de Ronde JJ, et al. Neoadjuvant chemotherapy in ER+HER2– breast cancer: response prediction based on immunohistochemical and molecular characteristics. *Breast Cancer Res Treat*. 2012;131:827–836.
28. de Ronde JJ, Hannemann J, Halfwerk H, et al. Concordance of clinical and molecular breast cancer subtyping in the context of preoperative chemotherapy response. *Breast Cancer Res Treat*. 2010;119:119–126.
29. Hoetjes NJ, van Velden FH, Hoekstra OS, et al. Partial volume correction strategies for quantitative FDG PET in oncology. *Eur J Nucl Med Mol Imaging*. 2010;37:1679–1687.
30. Tseng J, Dunnwald LK, Schubert EK, et al. ^{18}F -FDG kinetics in locally advanced breast cancer: correlation with tumor blood flow and changes in response to neoadjuvant chemotherapy. *J Nucl Med*. 2004;45:1829–1837.
31. Hatt M, van Stiphout R, le Pogam A, Lammering G, Visvikis D, Lambin P. Early prediction of pathological response in locally advanced rectal cancer based on sequential ^{18}F -FDG PET. *Acta Oncol*. August 8, 2012 [Epub ahead of print].
32. Hatt M, Le Pogam A, Visvikis D, Pradier O, Cheze le Rest C. Impact of partial volume effects correction on the predictive and prognostic value of baseline ^{18}F -FDG PET images in esophageal cancer. *J Nucl Med*. 2012;53:12–20.
33. Geets X, Lee JA, Bol A, Lonneux M, Gregoire V. A gradient-based method for segmenting FDG-PET images: methodology and validation. *Eur J Nucl Med Mol Imaging*. 2007;34:1427–1438.
34. Belhassen S, Zaidi H. A novel fuzzy C-means algorithm for unsupervised heterogeneous tumor quantification in PET. *Med Phys*. 2010;37:1309–1324.



The Journal of
NUCLEAR MEDICINE

Comparison Between ^{18}F -FDG PET Image-Derived Indices for Early Prediction of Response to Neoadjuvant Chemotherapy in Breast Cancer

Mathieu Hatt, David Groheux, Antoine Martineau, Marc Espié, Elif Hindié, Sylvie Giacchetti, Anne de Roquancourt, Dimitris Visvikis and Catherine Cheze-Le Rest

J Nucl Med. 2013;54:341-349.

Published online: January 17, 2013.

Doi: 10.2967/jnumed.112.108837

This article and updated information are available at:

<http://jnm.snmjournals.org/content/54/3/341>

Information about reproducing figures, tables, or other portions of this article can be found online at:

<http://jnm.snmjournals.org/site/misc/permission.xhtml>

Information about subscriptions to JNM can be found at:

<http://jnm.snmjournals.org/site/subscriptions/online.xhtml>

The Journal of Nuclear Medicine is published monthly.
SNMMI | Society of Nuclear Medicine and Molecular Imaging
1850 Samuel Morse Drive, Reston, VA 20190.
(Print ISSN: 0161-5505, Online ISSN: 2159-662X)

© Copyright 2013 SNMMI; all rights reserved.

The logo for the Society of Nuclear Medicine and Molecular Imaging (SNMMI) consists of the letters 'S', 'N', 'M', and 'I' arranged in a 2x2 grid. Each letter is white and set within a red square. To the right of this grid, the text 'SOCIETY OF NUCLEAR MEDICINE AND MOLECULAR IMAGING' is written in a black, sans-serif font, stacked in three lines.
SOCIETY OF
NUCLEAR MEDICINE
AND MOLECULAR IMAGING